R.I.S.T:

Radioulnar Instability Screening Tool

Progress Report

Group 24:

Saketh Balmoori

Kaitlyn Thornton

Chris Wissmann

11/26/2024

Page Count: 15

Table of Contents

List of Figures and Tables

Project Modifications

The need statement and project scope remain unchanged from the previous report, as does the project schedule and organization of team responsibilities. Three significant changes have been made to the device's design specifications:

(1) Device dimensions were updated from < 20 x 20 x 20 cm to < 40 x 40 x 40 cm, as further refinement of the force application and measurement systems suggested that the original volume would be insufficient.

(2) Adjustability ranges for the actuation mechanism and palm rest have been explicitly specified. The actuation mechanism now accommodates wrist thicknesses from 2-8 cm with a minimum of 1 cm of clearance on either side, and the palm rest is horizontally adjustable along the arm in a 15 cm range.

(3) Specific regulatory requirements for the device design have been chosen. The design will comply with ISO 13485:2019, which provides medical device-specific quality management guidelines, ISO 14971:2016 which provides medical device safety and risk mitigation guidelines, and ISO 9001:2015 which provides broader device quality management assurances.

All other design specifications remain fundamentally unchanged, but detailed metrics have been added where applicable. All design specifications are organized in *Table 1.1*, which can be found in *Appendix 1*, and the restated Need Statement and Project Scope can be found in *Appendix 3*.

Design Options

Throughout the iteration and brainstorming process, the design of the device has been subcategorized into four key areas: Actuation Mechanism - how force is applied to the DRUJ; Translation Measurement - how displacement of the ulna is measured in-response to applied force; Force Measurement - how applied forces are measured;

Main Rig Body - how the device is structured or packaged. Approaches and considerations for each of these categories are detailed below. Pugh Charts were constructed for the analysis of each of the main design categories using determined criteria. Each criteria was weighted a particular amount based on its degree of importance in the wider design; with higher scores reflecting better performance for that metric (less complex, cheaper, highly adjustable, etc.). This same basic analysis was conducted for all major design categories, though the number of design criteria and their weightings varied by group. Abbreviated Pugh Charts displaying the three highest-ranked criteria for the three highest-ranking solutions are placed throughout the text, with the total score across all criteria for each solution at the bottom of the table. Explanations for these three criteria and a solution's ranking for each are also detailed in the main text. Refer to *Appendix 1* for the extended charts and scoring explanations for all the criteria.

Main Rig Body - Discussion

A series of design solutions were considered for the Main Rig Body. The decision of the Main Rig Body, given the particular solutions ideated, played a significant role in influencing the alternatives created for all following design categories; as such, this design category was the most important to finalize. Details and analysis of each alternative are given below.

Gauntlet: A gauntlet was the first rig body concept. Fashioned similarly to heavy-duty braces worn throughout the fracture healing process, a robust bracer would be secured around the patient's limb. Actuation and measurement devices would be mounted directly to the gauntlet's surface to take recordings, before the gauntlet was doffed and donned on the patient's other arm.

External Glove: Decidedly "blue sky," this solution comprised a pair of electronic gloves to be worn by an examiner rather than hardware worn by the patient. The

gloves' fingertips would contain electromagnetic transducers to determine applied force, and inertial motion units would record displacement. Output data would be transmitted in real-time to a mobile app as the examiner performed the standard ballottement test, quantifying both the applied force and resultant translation.

Box + Bracer: The gauntlet idea was further adapted into a twofold system, wherein a stabilizing bracer is first fastened around the patient's limb and then secured into a larger chassis, or "box", which would contain the actuation mechanism and measurement systems, the latter of which could interface with aspects of the bracer.

Box (only): The final alternative involved a standalone chassis, or "box" with no external parts. The actuation mechanism and measurement systems, along with all necessary control hardware, would be fully contained within the box. Padded rests for the palm and proximal forearm fitted with hook-and-loop securing straps would rigidly fix a patient's limb into the device.

Main Rig Body - Analysis

Nine design criteria were highlighted for this category. *Rigidity* and *Measurability* were the two most crucial design aspects; *Rigidity* ensures translational measurements are noise-free, and *Measurability* is a general indication of how integrable measurement schemes are for a particular rig body. *Ejectability* and *Adjustability* were the next most-weighted criteria, with the former pertaining to ease of limb removal in case of emergency. *Complexity* was ranked next highest, pertaining to the number of static and dynamic components associated with a particular design solution. *Packaging*, *Comfort*, and *Cost* were all ranked next with equal weights. Though the client provided general specifications on desired device dimensions, no further constraints were applied beyond being able to accommodate a range of limbs. *Comfort* is key for maximizing patient compliance, especially given the potential of force application to induce pain in damaged wrists. *Cost* was ranked

relatively low, with the singular constraint of keeping prototype development costs below $1000. *Weight* was the lowest-ranked design criteria; while minimizing weight is useful for portability, particular solutions should be heftier in order to minimize extraneous motion that could induce noise during testing. *Table 1* has the numerical scores for the top three criteria, while *Table A1.2* has numerical scores for all criteria.

Table 1: Main Rig Body - Abbreviated Pugh Chart

Criteria	Weight	External Glove	Box	Box + Bracer
Measurability	10	5	8	8
Rigidity	10	1	9	10
Adjustability	9	10	9	6
	Total	**455**	**495**	**400**

The Box and Bracer combination scored highest for *Rigidity* due to constraining the entirety of the patient's limb prior to rigidly locking it to the chassis structure. It also scored the highest for *Measurability* alongside the isolated Box solution due to the significant increase in available dimensions to integrate various measurement schemes. Meanwhile, the External Glove solution scored highest for *Adjustability* since it forgoes any patient-attached hardware. Summing the scores for each criteria resulted in the singular Box ranking highest overall, even though the External Glove scored highest in the most categories. However, for the criteria in which it did not score the highest, it scored low due to the high costs for such small hardware, the lack of static fixation for patient limbs, and the lack of consistent translation and force measurability. Ranking as the lowest alternative for these three categories hampered the solution's final score. Detailed scoring for criteria and design options not shown in *Table 1* can be found in the *Main Rig Body* section of *Appendix 1*.

Actuation Mechanism – Discussion

Three design approaches were considered for the actuation mechanism, and are illustrated in *Figure 1.1*.

Rotational Eccentric Cams: The rotational eccentric cam system, *Figure 1.1, A*, was the first design concept for force application to the DRUJ. Rotational cams have a number of benefits: simplified packaging constraints due to the solely rotational motion of the cams, gradual, comfortable force application due to variable surface area, and being easily customizable in shape. This last property, in particular, would allow for the optimization of cam shape for adequate radial pinching. Finally, rotating eccentric cams can be used for bone translation in all desired hand positions: pronation, supination, and neutral.

Linear Transducers: *Figure 1.1, B* is an alternative to the eccentric cam system, instead using linear transducers for force application. Benefits of this system include: ease in determining force applied, high degree of adjustability for various wrist sizes and bone separation distances, control simplicity with the plug-and-play nature of transducers, and their applicability for all hand positions except for neutral. Furthermore, while a cam system is primarily limited to servo motor control, transducers using a pneumatic or hydraulic system for even more precise actuation and variable force ranges were considered due to the linear nature of desired motion.

Dual Clamp: Finally, a wrist clamp system (*Figure 1.1, C*) was also considered following a literature review of a DRUJ instability study using a rudimentary and inaccurate clamp setup [7]. This system would reduce the number of moving parts in the device, would provide the most secure radial mounting when used with padding, and still allows for pronation and supination measurements of either hand.

Actuation Mechanism – Analysis

Eight total criteria were outlined to judge the three mechanisms. For this group of designs, *Data Acquisition*, *Adjustability*, and *Contact Stability* were deemed most important; data should be simple to extract for real-time processing, actuators should accommodate a wide variety of wrists without losing accuracy, and patient limbs should be statically mounted to minimize measurement noise. *Safety* was highlighted as the next most important factor; given that the device is intended to diagnose wrist dysfunctions, doing so should not further exacerbate their condition. *Packaging Dimensions* and *Dynamic Complexity* are the next highest-ranked criteria. The former is key to maintaining device dimensions within specifications, while the latter pertains to the overall complexity of the motive mechanism; simpler mechanisms lead to fewer points of failure. *Limb Positions* and *Cost* were the lowest-ranked criteria. While a variety of limb positions does allow for a greater deal of measurement diversity, the clients advised that pronation is preferred. Meanwhile, cost was not prioritized as much as the other aspects of the design. Though not officially described, pneumatic and hydraulic options were disregarded due to low scores in *Cost*, *Dynamic Complexity*, and *Safety*. *Table 2* has the numerical scores for the top three criteria, while *Table A1.3* has numerical scores for all criteria.

Table 2: Actuation Mechanism – Abbreviated Pugh Chart

Criteria	Weight	Rotational Cams	Linear Transducers	Dual Clamp
Data Acquisition	10	3	8	2
Adjustability	10	4	10	6
Contact Stability	10	7	4	10
	Total	**455**	**495**	**400**

Transducers were also deemed the best for *Data Acquisition* due to the simplicity of recording linear displacement, as well as the consistent area of application on the transducer compared to the clamp. However, linear transducers won out on *Adjustability* due to the cams having limited vertical compliance, and the clamps being optimized for particular sizes. However, this optimization also means that clamps scored the best in *Contact Stability*. Summing the scores for each criteria resulted in the linear transducers ranking highest. Detailed scoring for criteria and design options not shown in *Table 2* can be found in the *Actuation Mechanism* section of *Appendix 1*.

Translation Measurement - Discussion

Due to the invasive nature of conventional bone translation measurements in literature considering the DRUJ [1,4], numerous alternatives were discussed for measuring resultant ulnar translation. Pivotal to this conversation was the involvement of Soft Tissue Artifacts (STAs) in the majority of noninvasive modalities. Given the clinical limitations preventing direct tracking of bone displacement via invasive electromagnetic tracking sensors, most sensing modalities must factor in the mechanical contributions of surrounding skin and soft tissue, including tendons, ligaments, fat, and nerves. Bulk measurements of arm translation resulting from applied force do not necessarily indicate isolated bone movement, as forces in a particular range may only result in the soft tissue being displaced. This serves as an even more critical issue when considering the difference in anatomy between the dorsal and volar sides of the arm, wherein differing musculature can contribute to mitigating bone displacement. Of the modalities considered, the seven most-developed are highlighted here, with two different combinations of sensing schemes also discussed for use in conjunction with Kalman filtering.

Ultrasound: Ultrasound provides one of the few literature-based tracking schemes for DRUJ stability quantification [8,9]. A makeshift setup combining a force transducer with ultrasound was used in a research setting, where ultrasound recorded an axial cross-section of a subject's limb. The change in distance between bony landmarks induced by compression of the ulna was recorded to a high degree of accuracy without significant computational cost.

Cuff-Mounted: The next two tracking mechanisms were coupled to the *Box + Bracer* alternative conceived for the device's *Main Rig Body*. Two possible tracking methods would be attached to the bracer using conventional fasteners or magnetic pads. One scheme involved a removable pad of plastic coated in a retroreflective material. The retro-reflective coating would be interspersed with bare plastic, effectively creating strips with a known width and spacing. As force is applied to the arm, the pad would translate up or down. Laser sensors mounted to the rig on either side would record the number of voltage pulses as the reflective pad moved, thus enabling calculation of bone displacement. A variant of this system replaced the laser sensors with Hall Effect sensors and the retro-reflective coating with a magnetic version. In essence, the system recorded translation in the same way, with a known width and spacing of magnetic material eliciting voltage pulses. Both tracking systems aimed to place the removable pad as close to the point of actuation as possible, though pads and their respective sensors could be translated across a portion of the rig's width if desired.

Structured Light: Structured light was another considered alternative, requiring a coupled projective light source and 3D vision scanning system. A grid pattern of optical light would be projected across the patient's limb from dorsal and axial views. The resultant light pattern deformation stemming from limb deformation would be used to recreate surface and depth scans of the joint. Invisible structured light was

considered in order to have two grid patterns, with one scanner and projector system focused on infrared light. Structured light in particular stands out as a non-radiative method for measuring geometries, mitigating safety concerns associated with ionizing scanning technologies.

IR Markers: A fully infrared tracking system was considered through the application of IR-reflective skin markers. Four IR sensors would be mounted around the limb: two above and two below, with two positioned in front of the actuation point and two behind it. This arrangement would enable tracking of eight skin-mounted reflector clusters. Clusters would be composed of three reflectors, using the pisiform bone's prominent jut as a landmark for aligning cluster locations. Once the radius has been pinched into place, the IR sensors on the ulnar side would record the distance to their pair of reflector clusters, averaging out the distances among the three markers in each cluster. This would inform the system of the wrist's nominal thickness, with the resultant wrist thickness measured after the final force has been applied. By subtracting out the approximate compression of skin and tissue by the force applicator from the nominal length, and then subtracting the nominal length from final length, approximate bone translation could be determined.

Software Rigidification: An additional factor can also be applied to any of the previous methods utilizing skin-mounted markers known as software rigidification. This method leverages an interpolation algorithm by using two time-separated sets of spatial recordings, highlighting prominent limb landmarks and overall limb posture [3]. A natural neighbor's interpolation algorithm can be used by feeding pre-recorded data of skin-mounted markers in relation to location of the bone, producing a transformation matrix that can be applied to videos of bulk limb deformation to isolate bone displacement. Crucially, this algorithm can be generally applied to rigid members attached to soft material matrices [3].

Actuator Translation Tracking (ATT):

The final mode of translation measurement involves a particular option highlighted in the proceeding Force Measurement section; force resistive sensors (FRS). Once the desired force direction and hand position are selected, two actuators will converge on the limb to pinch it. Prior to applying full pinching force, these actuators will converge until the sensor registers skin contact to determine the calibration distance. A pinching displacement is separately recorded while full pinching force is determined from FRS output. As the sensor records more pressure, its resistance will decrease, declining severely once rigid bone is reached. The difference between sequential resistance values is taken, with the actuators pausing once the resistive differences pass a certain hard-coded threshold. Finally, the translating actuator will push into the wrist until the desired force output is reached, at which point the final displacement will be recorded. By approximating the STA as negligible due to compressive forces from actuation, the prior calibration and pinching displacements are subtracted from the final displacement; this difference approximately yields total ulnar translation. This method has been termed the Actuator Translation Tracking method (ATT). The final measurement options combine ATT with either Optical Tracking or the bracer-mounted Hall Effect idea using a Kalman filtering process to finally average results from both systems as net ulnar translation [2].

Translation Measurement - Analysis

Nine design criteria were highlighted for the different translation measurement approaches. *Accuracy* is weighted the highest, given the device's focus on gathering results comparable to the highly-invasive gold standard. *Feedback Delay* was ranked of similar importance for real-time measurements of force and displacement. *Hardware Complexity* and *Patient Prep Time* are the next highest ranked, as complex

hardware would strain development capacity while preparation time would affect testing efficiency. *Cost* and *Sampling Rate* were equally weighted as the next lowest, with *Cost* reflecting hardware expenses and *Sampling Rate* tied to measurement accuracy. *Software Complexity* was ranked lower given the group's development experience, followed by *Computational Requirements*, while *Power Requirements* ranked lowest overall. Accuracy was generally preferred even if schemes were computationally complex. *Table 3* has the numerical scores for the top three criteria, while *Table A1.4* has numerical scores for all criteria.

Table 3: Translation Measurement - Abbreviated Pugh Chart

Criteria	Weight	Ultrasound	IR Markers	FSAIC
Accuracy	10	9	6	6
Feedback Delay	10	9	8	9
Hardware Complexity	9	8	7	8
	Total	418	430	537

Ultrasound scored highest on *Accuracy*, alongside IR Markers. Ultrasound scored similarly to ATT for *Hardware Complexity*; ATT uses rudimentary sensors and mounting solutions with no extra moving parts, whereas Ultrasound would be used in a prepackaged portable wand format. Finally, ATT and Ultrasound ranked the highest for *Feedback Delay* due to the simple calculations required for the latter and the nature of how the former records information. Summing the scores for each criteria resulted in ATT ranking highest overall. Detailed scoring for criteria and design options not shown in *Table 3* can be found in the *Translation Measurement* section of *Appendix 1*.

Force Measurement – Discussion

The other desired datum is the force applied by the selected actuators. Three different approaches for measuring the applied force were considered.

Force-Resistive Sensors: The first approach is force resistive sensors (FRS), which can be adhered to actuator contact surfaces, outputting an analog voltage signal as increasing forces reduce the impedance of the sensor's resistive element. Linearizing with known forces allows for registering sensor data exactly at the point of contact with the limb. Further characteristic changes in resistance feedback after limb contact has been made can also indicate when maximal soft tissue deformation has been achieved, and thus when bone has been contacted.

Strain Gauges: Alternatively, strain gauges can be attached to the contact surfaces of actuators, providing a degree of separation between the limb and the actuators; yet due to being series elements in the mechanical circuit, they should have no bearing on final force output while enabling highly accurate force readings.

Current Back-Calculation: Back-calculating from input current driving the actuating mechanism provides another force measurement method with no additional hardware requirements. Given that fundamental servo properties such as torque constants, actuation speed, and the torque response curve are known for a chosen servo, specific input currents can be delivered to elicit desired force outputs from the actuator. This system would then rely on nominal forces rather than a method of gauging actively applied ones.

Force Measurement – Analysis

Eight design criteria were highlighted for the force measurement alternatives. *Accuracy* was once again taken as the most important metric due to the small force ranges employed for DRUJ diagnostics. *Feedback Delay* was weighted similarly to the Translation Measurement category for the same reasons detailed in the prior section. *Hardware Complexity* was the next highest-weighted criteria on the basis

that design simplicity reduces potential modes of failure. *Cost* and *Sampling Rate* were also weighted identically to the Translation Measurement category for the same reasons as above. However, *Packaging Dimensions* was also weighted the same as these two criteria. Any useful force measurement scheme would need to be in-line with the application method; as such, smaller form factors are desired in order to constrain device dimensions. *Software Complexity* and *Computational Requirements* were the two lowest-weighted criteria, as with the previous measurement design category. *Table 4* has the numerical scores for the top three criteria, while *Table A1.5* has numerical scores for all criteria.

Table 4: Force Measurement - Abbreviated Pugh Chart

Criteria	Weight	Strain Gauge	Force-Resistive Sensor	Current Back-Calculation
Accuracy	10	10	8	6
Feedback Delay	10	10	7	6
Hardware Complexity	9	7	8	10
	Total	483	497	478

The strain gauge scored highest for *Accuracy* and *Feedback Delay* due to its high fidelity and responsiveness. Current back-calculation was rated highest for *Hardware Complexity* as it requires no extra components beyond the actuators. Summing the scores for each criteria resulted in FRS ranking highest overall. Detailed scoring for criteria and design options not shown in *Table 4* can be found in the *Force Measurement* section of *Appendix 1*.

Chosen Design

The best-scoring approaches in each design category (Box, Linear Transducers, ATT, Force-Resistive Sensors) were combined into a comprehensive package for the R.I.S.T, which is illustrated in *Figure A2.1*. Physical dimensions, material selection, and assembly for the device are detailed here, however system architecture, actuator control logic, and additional supplementary figures can be found in *Appendix 2*.

Chassis: The device's main structure is an extruded aluminum chassis (20 cm x 20 cm x 48 cm), with members conjoined by machined aluminum brackets using T-slot fasteners. Two 3.175 mm thick aluminum crossbars span the chassis' width, providing additional support for the actuation assembly.

Transducer Mounting: Four linear transducers are mounted in two vertically aligned pairs with force-resistive sensors on 3D printed inserts. The printed inserts contact limit switches positioned at the end of the transducer body when transducers are maximally retracted, serving as system endstops. Each transducer is housed in a 3D-printed carriage that moves along a lead screw. Chrome-plated C45 steel motion rods parallel to the lead screws support the carriage assemblies. Trapezoidal 3D-printed brackets with bearings retain the motion rods and lead screws.

Transducer Adjustability: On the outside of the external brackets, 3D-printed cranks are attached to each of the lead screws and are connected vertically by a 3.175 mm thick aluminum bar. Each pair of cranks is driven by a single knob, enabling horizontal adjustment of the corresponding transducer pair while maintaining vertical alignment.

Limb Rests: A 7.76 cm segment of extruded aluminum extends upward from the center of the rear lower horizontal chassis member, with another 8 cm extruded aluminum segment fixed horizontally atop the previous, extending backward. A 4 cm x 8 cm x 3.175 mm aluminum plate is fastened to the horizontal aluminum member,

upon which a 7.13 cm thick faux-leather wrapped block of PVC foam and a hook-and-loop fastening strap are mounted, creating a rest for the proximal forearm. Two 15 cm square aluminum telescoping tubes mounted 12.8 cm high on the front vertical chassis members support a 20 cm extruded aluminum member with an identical padded aluminum plate mounted at the center, comprising the palm rest.

Component Mounting: A 3.175 mm aluminum plate is attached to the inside face of the lower front horizontal cross member, forming a bracket to which a 12V 5A DC power supply is mounted. Another 3.175 mm aluminum plate is fixed to the outside face of the upper front horizontal cross member. An Arduino Uno and servo controller are mounted to the plate with standoffs. An LCD control panel with an integrated knob and button is fixed into a 3D printed shell that bolts to the plate, protecting the electronics.

Proposed Budget

The current estimated subtotal for the R.I.S.T device and all components is $991.66. Our clients are willing to provide up to $1000 in funding, meaning that the current estimate is within limits. However, efforts are still ongoing to reduce costs to provide breathing room for production setbacks, shipping, and other possible expenses. *Table A3.1* provides a detailed overview of the current budget. Actuation comprises $424.91, Translation Measurement comprises $19.80, Chassis comprises $333.54, Electronics comprises $133.41, with the remaining accounting for the last $100. The $1000 price range for the R.I.S.T prototype is significantly lower than existing alternatives, and was also recommended by the clients as a maximum limit for market viability. An explanation of notable expenditures can be found accompanying *Table A3.1* in the third Appendix.

References

[1] Ancillao, A., Aertbeliën, E., & De Schutter, J. (2021). Effect of the soft tissue artifact on marker measurements and on the calculation of the helical axis of the knee during a gait cycle: A study on the CAMS-Knee data set. Human movement science, 80, 102866. https://doi.org/10.1016/j.humov.2021.102866

[2] Becker, A. (2024) Kalman Filtering. An Overview. kalmanfilter.net

[3] Bouvel, S., Pasqui, V., & Morel, G. (2015). Validation of a new method for bone motion measurement by soft-tissue artifact compensation through spatial interpolation. In 2015 IEEE/RSJ International Conference on Intelligent Robots and Systems (IROS) (pp. 2611-2616). IEEE.

[4] Fiorentino, N. M., Atkins, P. R., Kutschke, M. J., Goebel, J. M., Foreman, K. B., & Anderson, A. E. (2017). Soft tissue artifact causes significant errors in the calculation of joint angles and range of motion at the hip. Gait & posture, 55, 184–190. https://doi.org/10.1016/j.gaitpost.2017.03.033

[5] Gordon, C. C., Blackwell, C. L., Bradtmiller, B., Parham, J. L., Barrientos, P., Paquette, S. P., Corner, B. D., Carson, J. M., Venezia, J. C., Rockwell, B. M., Mucher, M., & Kristensen, S. (2012). 2012 Anthropometric Survey of U.S. Army Personnel: Methods and Summary Statistics (Report No. NATICK/TR-15/007). U.S. Army Natick Soldier Research, Development and Engineering Center.
http://tools.openlab.psu.edu/publicData/ANSURII-TR15-007.pdf

[6] Mukohara, S., Mifune, Y., Inui, A., Nishimoto, H., Kurosawa, T., Yamaura, K., ... & Kuroda, R. (2021). A new quantitative evaluation system for distal radioulnar joint instability using a three-dimensional electromagnetic sensor. Journal of Orthopaedic Surgery and Research, 16, 1-10.

[7] Pickering, G. T., Nagata, H., & Giddins, G. E. (2016). In-vivo three-dimensional measurement of distal radioulnar joint translation in normal and clinically unstable populations. The Journal of hand surgery, European volume, 41(5), 521–526. https://doi.org/10.1177/1753193415618110

[8] Yoshii, Y., Yuine, H., Tung, W. L., & Ishii, T. (2019). Quantitative assessment of distal radioulnar joint stability with pressure-monitor ultrasonography. Journal of orthopaedic surgery and research, 14(1), 195. https://doi.org/10.1186/s13018-019-1237-3

[9] Yuine, H., Yoshii, Y., Iwai, K., Ishii, T., & Shiraishi, H. (2022). Application of force-monitor ultrasonography to assess distal radioulnar joint instability in patients with triangular fibrocartilage complex injury. Ultrasound (Leeds, England), 30(3), 219–227. https://doi.org/10.1177/1742271X211038351

Appendix 1

Updated design specs for the device and all material pertaining to *Design Options* including figures, full Pugh Charts, and explanations of criteria and design options not present in the main body text, are contained in Appendix 1.

Table A1.1: Updated Device Specifications

Category	Sub-Category	Specification
Performance	Sensitivity	< 0.5 mm joint displacement
	Force Application	customizable, 0-20 N range with 0.25 N resolution
	Force Application Lag Time	Input-to-actuation lag time of < 1 s
	Software Sampling Rate	> 100 samples/sec
	Software Lag Time	Real-time force and translation output
Accessibility & Ergonomics	Testing Setup Comfort	Arm setup in chassis is comfortable for extended testing periods (> 10 min)
	Hand/Palm Rest	Adjustable horizontal (along arm) range of 15 cm.
	Limb Zone	Adjustable testing zone diameter of 10-25 cm
	Rig Chirality	Ambidextrous, capable of force application on dorsal and ventral sides of both wrists
Safety & Compliance	Device Material	Hypoallergenic
	Device Cleaning	Sanitizable in < 10 min
	Arm Removal	Limb removal in < 15 s in event of emergency
	Physical Emergency System	Manual shut-off switch in event of patient discomfort
	Software Emergency System	Software shut-off switch in event of wrist displacement exceeding 4.81 cm of translation
	Regulatory Standards	ISO 13485:2019, ISO 14971:2016, and ISO 9001:2015 compliant

Table 1.1: Updated Device Specifications (continued)

Category	Sub-Category	Specification
Technical Design	Sensor Implementation	Non-invasive
	Sensor Variability	Calibratable for wrist thicknesses within 2-8 cm [5]
	Mechanical Isolation	Chassis vibrationally isolated from ambient, <0.1 mm of chassis movement
	Electrical Isolation	Chassis grounded and patient electrically isolated
	Device Dimensions	$<$ 40 x 40 x 40 cm
	Arm Mounting System	Two-point mounting, arm must remain entirely static prior to force application
UI & Operation	Operational Regulations	Easy operation, learning period <1 hr
	Display	Simple digital display for real-time force/translation readout
	Interactive Operability	Large, tactile buttons, dials, and/or switches
	Data Output	universally recognized by any modern computer
Prototype Development Cost		$<$\$1000

Pugh charts and any other visualizations for each of the design's four key subcategories – Main Rig Body, Actuation Mechanism, Translation Measurement, and Force Measurement – are collected here. Scoring criteria and design alternatives not discussed in the main body text are also provided.

Main Rig Body

Four options were considered for the Main Rig Body, and are detailed in *Table 1.2*.

Table A1.2: Main Rig Body - Pugh Chart

Criteria	Weight	Gauntlet	External Glove	Box	Box + Bracer
Measurability	10	3	5	8	8
Rigidity	10	2	1	9	10
Adjustability	9	2	10	9	6
Ejectability	9	4	10	8	6
Complexity	8	2	9	5	4
Comfort	7	5	9	7	6
Cost	7	3	1	8	7
Packaging	7	8	10	6	3
Weight	5	6	9	2	2
	Total	**262**	**497**	**520**	**442**

The External Glove solution scored highest for *Ejectability* and *Comfort* since it forgoes any patient-attached hardware. The glove also scored the highest for *Complexity* and *Packaging* due to its lack of moving parts and comparatively minimal volume: also dominating for *Weight* for the same reasons. Finally, the isolated Box solution scored the highest for *Cost* due to allowing for larger and cheaper hardware and electronics while also being one major component.

Actuation Mechanism

Three design options were considered for the actuation mechanism, An axial view of each is depicted in *Figure A1.1*, and detailed scoring is given in *Table A1.3*.

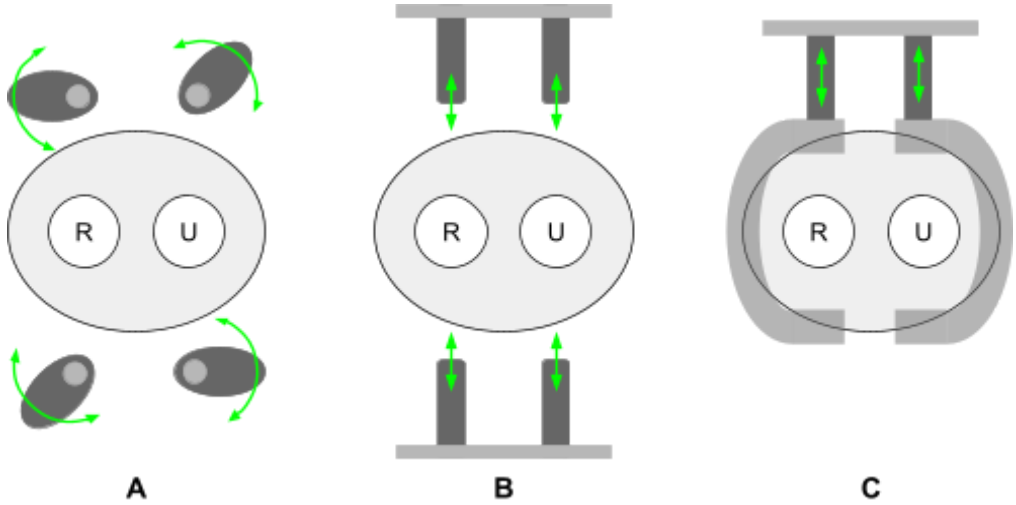

Figure A1.1: Design approaches for actuation mechanism.
A = rotational eccentric cams, B = linear transducers, C = actuating dual-clamp.
Distal axial view of the left hand in pronation. R = radius, U = ulna.

Table A1.3: Actuation Mechanism - Pugh Chart

Criteria	Weight	Rotational Cams	Linear Transducers	Dual Clamp
Data Acquisition	10	3	8	2
Adjustability	10	4	10	6
Contact Stability	10	7	4	10
Safety	9	7	9	4
Packaging Dimensions	8	9	4	6
Dynamic Complexity	8	5	8	3
Limb Positions	7	10	8	8
Cost	7	10	6	8
	Total	455	495	400

Linear transducers ranked highest for *Safety*, given their ease of retractability and slow actuation speed; a clamp system would be difficult to separate from the patient, and the rotational motion of cams limits their retractability. However, the smaller dimensions of cams as well as the minimal space needed for cam displacement compared to the range of motion for clamps or transducers led to their high ranking for *Packaging Dimensions*. Transducers scored highest on *Dynamic Complexity* due to their well-characterized motion, whereas the off-axis force application of the clamps and the difficulty in verifying cam position reduced their *Dynamic Complexity* scores. Rotational cams were deemed better for accommodating more *Limb Positions* as their application is not restricted along an axis. Finally, cams scored highest on *Cost* due to the cheap nature of 3D printing robust eccentric cams.

Translation Measurement

The seven most considered design options for translation measurement are detailed in *Table A1.4*.

Table A1.4: Translation Measurement - Pugh Chart

Criteria	Weight	Ultrasound	Optical Cuff	Hall-Effect Cuff	Structured Light	IR Markers	Software Rigidification	ATT
Accuracy	10	9	2	4	7	6	9	6
Feedback Delay	10	9	5	5	2	8	4	9
Hardware Complexity	9	8	8	8	3	7	4	8
Patient Prep Time	9	3	6	6	10	4	10	10
Cost	7	1	6	6	2	8	3	10
Sampling Rate	7	10	7	7	3	9	3	8
Software Complexity	6	7	9	9	2	7	2	9
Computational Requirements	5	4	9	9	2	6	3	9
Power Requirement	4	5	8	8	4	7	3	8
	Total	418	386	406	264	430	325	537

The simplicity and low cost of force-resistive sensors led ATT to score the highest on *Cost* while both cuff options scored similarly to Ultrasound and ATT for *Hardware Complexity*; the cuff options also use rudimentary sensors and mounting solutions with no extra moving parts. Both cuff options and ATT also scored the

highest on *Computational Requirements* due to simple sensors. However, only ATT and the cuff options scored the highest for *Software Complexity* since ultrasound would require an external computer and proprietary recording software. All three also scored the highest for *Power Requirements* due to their simple sensors. Structured Light, ATT, Software Rigidification, and the Optical solutions scored equally high on the *Patient Prep* metric as none of these measurement schemes require hardware mounted on the patient or alternative preparation, unlike ultrasound. Ultrasound scored the highest for *Sampling Rate* due to its ability to capture thousands of frames per second.

Force Measurement

The three main options considered for force measurement are detailed in *Table A1.5*.

Table A1.5: Force Measurement - Pugh Chart

Criteria	Weight	Strain Gauge	Force-Resistive Sensor	Current Back-Calculation
Accuracy	10	10	8	6
Feedback Delay	10	10	7	6
Hardware Complexity	9	7	8	10
Cost	7	4	9	10
Sampling Rate	7	10	8	9
Packaging Dimensions	7	4	9	10
Software Complexity	6	9	8	5
Computational Requirements	5	8	9	7
	Total	483	497	478

The strain gauge also scored highest for *Sampling Rate* due to its high fidelity and responsiveness. Current back-calculation was rated highest for *Cost* and *Packaging Dimensions*, due to requiring no extra components. The strain gauge system scored highest on *Software Complexity* due to requiring minimal calculations compared to the other options for force feedback. Finally, FRS scored the highest for *Computational Requirements* due to the simplicity of its analog feedback compared to strain gauges and simpler calculations compared to the current back-calculation solution. Summing the scores for each criteria resulted in FRS ranking highest overall.

Appendix 2

All supplementary materials for the R.I.S.T's chosen design are present in this Appendix. A preliminary CAD rendering of the chosen design is illustrated in *Figure A2.1*.

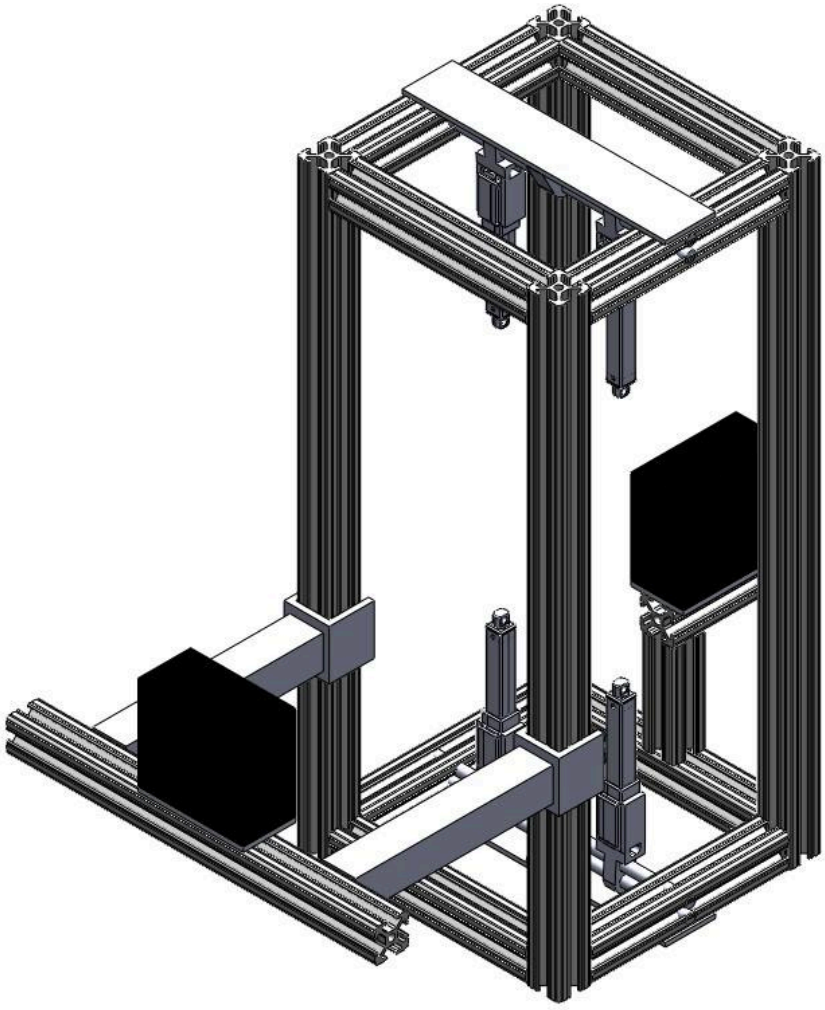

Figure A2.1: R.I.S.T. preliminary CAD. Cranking linkages, fastening hardware, and system electronics not shown. Black boxes are dimensionally inaccurate representations of the palm and wrist rest padding.

Alongside preliminary CAD, notable consideration has been put into system design and control logic. A block diagram detailing the control and feedback scheme of the device is presented in *Figure A2.2*.

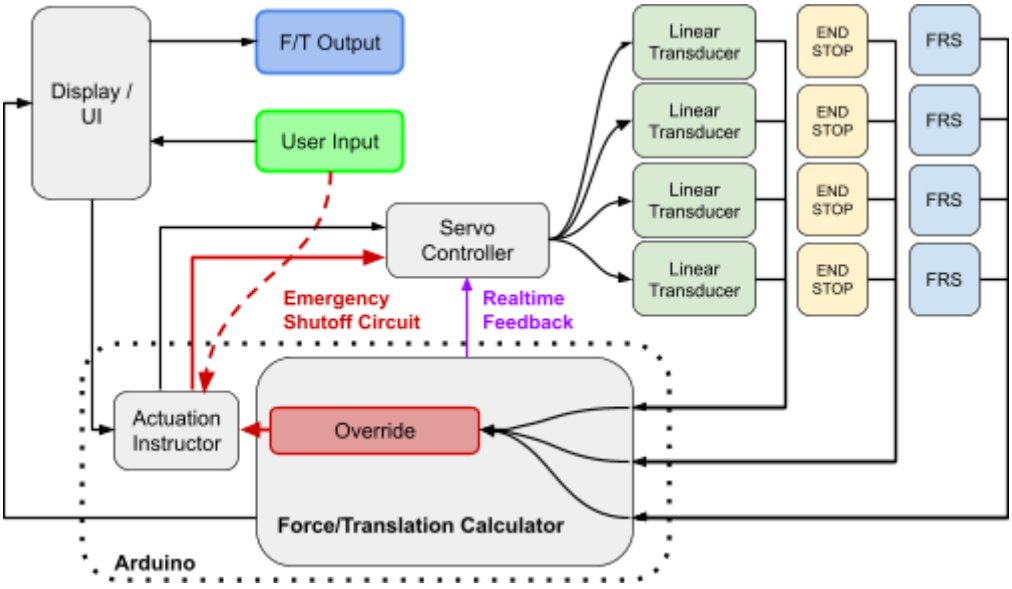

Figure A2.2: R.I.S.T. feedback and control scheme block diagram.

For normal operation, a user provides an input to the display, which is run by the "Actuation Instructor" Arduino program. Once the user has selected and confirmed the desired testing scheme, the Actuation Instructor sends predefined commands to the servo controller, executing the desired test. Output from the linear transducers, endstop switches, and FR-sensors are received by the "Force/Translation Calculator" program. These outputs are first checked by "Override," which ensures that no emergency shutoff thresholds have been crossed. Relevant positional/force information is returned to the servo controller, continuing the current test. The Force/Translation program then calculates the current ulnar translation and applied force, which are sent back to the display as outputs.

The user can also explicitly input a shutoff command, which bypasses the Force/Translation Calculator and Override, directly activating a pre-loaded abort sequence in the Actuation Instructor, causing each linear transducer to fully retract.

This same abort sequence is also activated if Override determines any force/displacement thresholds have been crossed.

Significant work has also been done to determine the exact nature of the instructions the Actuation Instructor program will provide to the servo controllers. Four possible hand positions exist for the chosen design: right hand in pronation (RP), right hand in supination (RS), left hand in pronation (LP), and left hand in supination (LS), with dorsal or volar load being applied in each, making eight total testing schemes. Considering the positions of the linear transducers to be static relative to the changing limb positions, the participatory transducers were determined for each of the eight testing schemes. An overview of the four hand positions and the resultant transducer configurations is given in *Figure 2.3*.

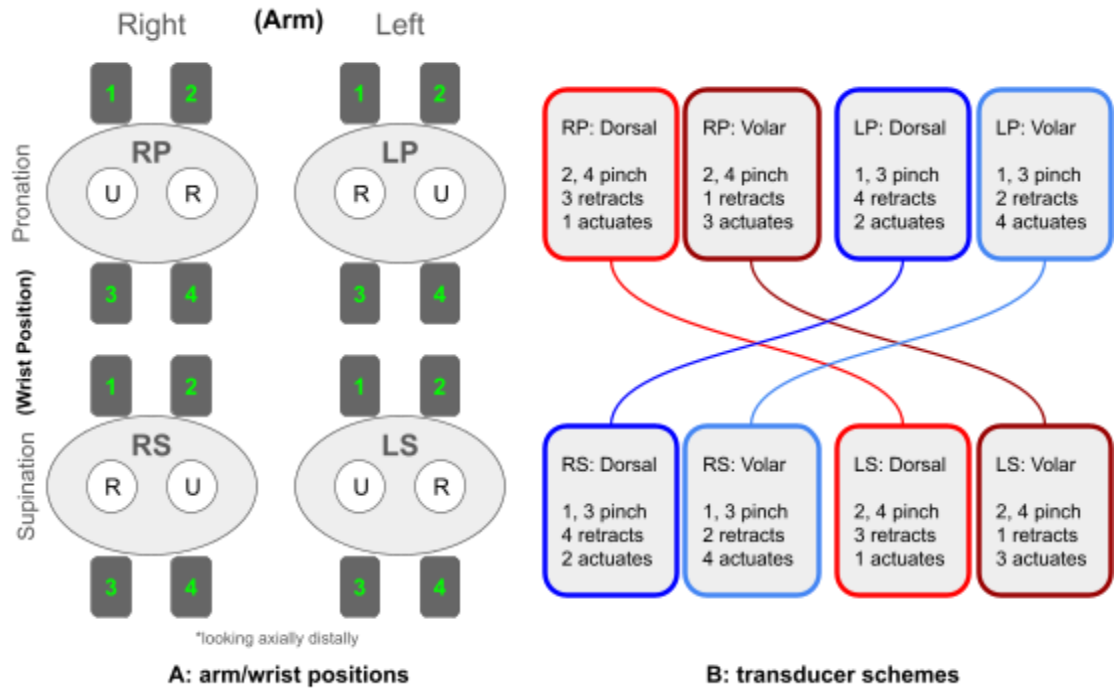

Figure A2.3: Overview of testing schemes. A = the four possible arm/wrist positions, B = written out transducer operation schemes for all possible testing conditions.

Analysis of *Figure 2.3, B* illustrates notable symmetry between transducer schemes. In both dorsal and volar force application, RP and LS are the same, as are LP and

RS. This symmetry reduces the total unique number of transducer schemes to four, however the inherent similarities between the unique schemes suggests that a single control program with parameterized inputs could handle all of the logic necessary to complete a given test. Pseudocode for such a program is shown in *Figure 2.4*.

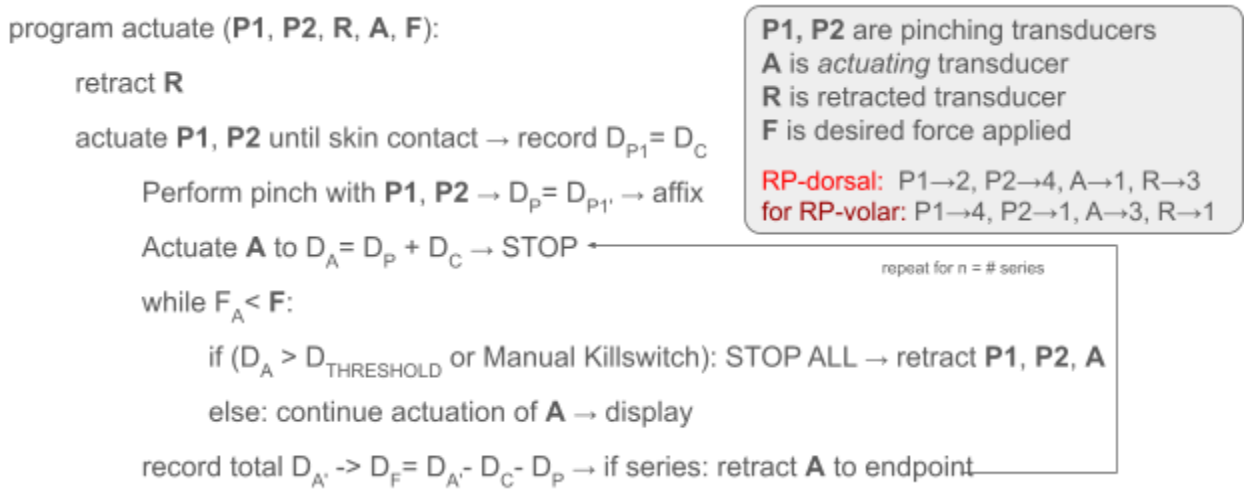

Figure A2.4: pseudocode for transducer control program

Although an exact implementation including particular sensor feedback has yet to be written, the general structure of the control code is evident in *Figure 2.4*. Ideally, this program would be flashed into the firmware of the servo controller itself, with inputs P1, P2, R, A and F being provided by the Actuation Instructor program, and force/displacement measurements being communicated between the servo controller and the Force/Translation Calculator Arduino program.

Appendix 3

Appendix 3 contains R.I.S.T's need statement and project scope, which remain unchanged from the previous report. The current budget, itemized in *Table 3.1* along with explanations for notable expenditures also reside in this Appendix.

Need Statement:

When orthopedic hand surgeons attempt to understand distal radioulnar joint instability, there is a need to efficiently and practically quantify joint stability to succinctly inform surgical decision-making for more favorable outcomes.

Project Scope:

Diagnosis of instability in the distal radioulnar joint is limited to a qualitative judgment of "stable" or "unstable;" efficient, practical assessment of distal radioulnar joint stability currently remains out of reach. Presently, qualitative wrist ballottement tests are used to elicit doctor opinion and patient pain response to determine structural instability. A rig involving drilling into the arm bones of cadavers to mount electromagnetic tracking sensors and a Microscribe transducer was used as an invasive, yet accurate method of instability quantification. With a similarly capable portable, noninvasive, and comfortable device, surgeons could better judge the surgical methodology required for an individual patient and reliably determine post-operative efficacy.

We intend to develop a non-invasive system to gauge joint instability by February 2025, and deliver a final prototype to Dr. Goldfarb by April 20th, 2025 so that his surgical team can gauge the system's accuracy and reliability in a clinical setting. Alongside prototype delivery, we will provide manufacturing plans and relevant design files needed to reproduce the rig in the event of success.

Table A3.1: Preliminary Itemized Budget

Item	Qty	Unit Cost	Item Subtotal
HiTec 50 mm linear servo actuator	4	$99.99	$399.96
6-channel servo controller	1	$24.95	$24.95
Force resistive sensor	4	$4.95	$19.80
Arduino Uno	1	$31.74	$31.74
Black anodized extruded aluminum bars	5	$21.15	$105.75
Prusa LCD unit	1	$56.72	$56.72
12V 5A PSU	1	$24.95	$24.95
Lead screws	4	$14.97	$59.88
Linear motion rods	8	$9.99	$79.92
Telescopic tubing locks	6	$6.00	$36.00
Square aluminum telescopic tubing, 1"	3	$8.92	$26.76
Square aluminum telescopic tubing, 0.875"	3	$8.41	$25.23
Hardware, Filament, Wiring, Consumables	N/A		$100.00
		Total	$991.68

Notable expenditures include: the linear transducers, the extruded aluminum bars, and the linear motion rods. These linear transducers were specifically highlighted for their optimal force output and actuation speed ranges, digital servo feedback, moderately-sized stroke length, discreet packaging, and actuator millimeter-scale markings. Extruded aluminum provides an easily workable, modular, and durable material platform to construct the chassis. Finally, linear motion rods are used in the mounting system of the transducers alongside lead screws to provide a highly adjustable horizontal range of motion while maintaining servo rigidity during actuation.